Available online at www.sciencedirect.com

SCIENCE DIRECT®

Developmental Biology 272 (2004) 310–327

DEVELOPMENTAL BIOLOGY

www.elsevier.com/locate/ydbio

Regulation of ureteric bud branching morphogenesis by sulfated proteoglycans in the developing kidney

Dylan L. Steer,[a,1] Mita M. Shah,[a,1] Kevin T. Bush,[a] Robert O. Stuart,[a] Rosemary V. Sampogna,[a] Tobias N. Meyer,[2] Catherine Schwesinger,[2] Xaiomei Bai,[3] Jeffrey D. Esko,[b] and Sanjay K. Nigam[a,b,c,*]

[a] *Department of Medicine, University of California, San Diego, La Jolla, CA 92093-0693, USA*
[b] *Department of Cellular and Molecular Medicine, University of California, San Diego, La Jolla, CA 92093-0693, USA*
[c] *Department of Pediatrics, University of California, San Diego, La Jolla, CA 92093-0693, USA*

Received for publication 10 February 2004, revised 16 April 2004, accepted 19 April 2004

Abstract

Glycosaminoglycans in the form of heparan sulfate proteoglycans (HSPG) and chondroitin sulfate proteoglycans (CSPG) are required for normal kidney organogenesis. The specific roles of HSPGs and CSPGs on ureteric bud (UB) branching morphogenesis are unclear, and past reports have obtained differing results. Here we employ in vitro systems, including isolated UB culture, to clarify the roles of HSPGs and CSPGs on this process. Microarray analysis revealed that many proteoglycan core proteins change during kidney development (syndecan-1,2,4, glypican-1,2,3, versican, decorin, biglycan). Moreover, syndecan-1, syndecan-4, glypican-3, and versican are differentially expressed during isolated UB culture, while decorin is dynamically regulated in cultured isolated metanephric mesenchyme (MM). Biochemical analysis indicated that while both heparan sulfate (HS) and chondroitin sulfate (CS) are present, CS accounts for approximately 75% of the glycosaminoglycans (GAG) in the embryonic kidney. Selective perturbation of HS in whole kidney rudiments and in the isolated UB resulted in a significant reduction in the number of UB branch tips, while CS perturbation has much less impressive effects on branching morphogenesis. Disruption of endogenous HS sulfation with chlorate resulted in diminished FGF2 binding and proliferation, which markedly altered kidney area but did not have a statistically significant effect on patterning of the ureteric tree. Furthermore, perturbation of GAGs did not have a detectable effect on FGFR2 expression or epithelial marker localization, suggesting the expression of these molecules is largely independent of HS function. Taken together, the data suggests that nonselective perturbation of HSPG function results in a general proliferation defect; selective perturbation of specific core proteins and/or GAG microstructure may result in branching pattern defects. Despite CS being the major GAG synthesized in the whole developing kidney, it appears to play a lesser role in UB branching; however, CS is likely to be integral to other developmental processes during nephrogenesis, possibly involving the MM. A model is presented of how, together with growth factors, heterogeneity of proteoglycan core proteins and glycosaminoglycan sulfation act as a switching mechanism to regulate different stages of the branching process. In this model, specific growth factor–HSPG combinations play key roles in the transitioning between stages and their maintenance.

Keywords: Heparan sulfate proteoglycan; Chondroitin sulfate proteoglycan; Kidney development; Ureteric bud; Branching morphogenesis; Organ culture; Isolated ureteric bud culture; Microarray

Introduction

Branching morphogenesis is a central feature of the developmental program of epithelial organs as diverse as kidney, lung, breast, liver, and pancreas, and results from a complex interaction between mesenchymal and epithelial components. In the developing kidney, studies with the isolated ureteric bud (UB) in culture suggest that the branching program is induced by the activation of cell surface receptors by soluble growth factors (Qiao et al.,

* Corresponding author. Department of Medicine (0693), University of California, San Diego, 9500 Gilman Drive, La Jolla, CA 92093-0693. Fax: +1-858-822-3483.
E-mail address: snigam@ucsd.edu (S.K. Nigam).
[1] These authors contributed equally to this work.
[2] Current address: Department of Medicine, Division of Nephrology, University of Hamburg, Martinistr. 52, 20246 Hamburg, Germany.
[3] Current address: Neose Technologies, Inc., San Diego, CA, USA.

0012-1606/$ - see front matter © 2004 Published by Elsevier Inc.
doi:10.1016/j.ydbio.2004.04.029

2001), and requires other regulated effectors of branching such as matrix proteases (and their inhibitors) (Pohl et al., 2000a). Proteoglycans (PG) have been identified as mediators of growth factor–receptor interactions and are also major constituents of the extracellular milieu (Perrimon and Bernfield, 2000); thus, they are likely to play key roles in the development of these organs.

Proteoglycans consist of a protein core coupled to unique, variably sulfated glycosaminoglycan (GAG) chains. Two types of GAG chains predominate, heparan sulfate (HS), or chondroitin sulfate (CS), and there appears to be a large degree of structural diversity within these chains based on variable sulfation and uronic acid composition. The HSPGs include the syndecan and glypican gene families, and the matrix proteoglycans perlecan, agrin, and collagen XVIII. Glypicans and syndecans are attached to the cell surface; syndecans are transmembrane proteins, while glypicans are glycosylphosphoinositide-linked proteins. Perlecan, agrin, and collagen XVIII proteoglycans are associated with basement membranes. A wide variety of growth factors and morphogens implicated in branching morphogenesis or other aspects of kidney development, such as FGFs (Allen et al., 2001; Clayton et al., 2001; Qiao et al., 2001), members of the TGFβ superfamily (Bush et al., 2004; Sakurai and Nigam, 1997; Santos and Nigam, 1993), GDNF (Barnett et al., 2002), pleiotrophin (Sakurai et al., 2001), BMPs (Bush et al., 2004; Grisaru et al., 2001), Wnts (Kispert et al., 1996), and hedgehog (The et al., 1999), interact with HS and often require this interaction for downstream signaling.

A role for HSPGs in development, and more specifically kidney development, has been demonstrated in studies involving genetically mutated mice. At several steps in the biosynthesis of HSPGs, mutations have been found that disrupt normal development (reviewed in Shah et al., 2004). For example, mice lacking Heparan sulfate 2-sulfotransferase (*Hs2st*), a gene that encodes an enzyme responsible for sulfating iduronic acid and glucuronic acid residues on HS, die in the neonatal period due to renal agenesis (Bullock et al., 1998; Merry et al., 2001). Mutations in the core proteins themselves also can lead to renal defects. Glypican-3-deficient mice exhibit developmental overgrowth, cystic and dysplastic kidneys, and defective lung development (Cano-Gauci et al., 1999). These features are similar to the human Simpson–Golabi–Behmel syndrome, which is caused by mutations in the Glypican-3 gene (Pilia et al., 1996). The role of CSPGs in kidney development has not been well characterized and an abnormal kidney phenotype has not been reported in the CSPG knockout mice generated thus far (reviewed in Ameye and Young, 2002).

The mammalian kidney or metanephros, arises through the interaction between the epithelial UB and the metanephric mesenchyme (MM). Through a series of reciprocal inductive events, the UB invades the mesenchyme and then undergoes multiple iterations of a branching program that leads to the development of an extensive urinary collecting system (reviewed in Bush et al., 2003; Pohl et al., 2000b; Steer et al., 2004; Shah et al., 2004). The MM condenses at the tips of UB branches and undergoes a mesenchymal-to-epithelial transition, thereby forming the nephron tubules associated with each collecting duct. Although many of the factors that initiate and control UB branching morphogenesis and mesenchymal transformation have been elucidated, the roles of sulfated proteoglycans in these disparate processes have not been clearly defined. Until recently, methods to study UB branching morphogenesis as a process distinct from surrounding MM differentiation were unsuccessful. However, it is now known that the UB can be isolated from the MM and cultured within a Matrigel/collagen extracellular matrix. When exposed to soluble growth factors and media conditioned by mesenchymal cells, the isolated UB enacts an elaborate branching program that is thought to be intrinsic to the UB (Qiao et al., 1999). This assay allows for the examination of direct effectors of UB branching morphogenesis independent from secondary mesenchymal influences (Bush et al., 2004; Qiao et al., 2001; Zent et al., 2001).

Several studies have indirectly suggested the importance of sulfated GAGs to kidney branching morphogenesis (Davies et al., 1995; Lash et al., 1983; Lelongt et al., 1988; Platt et al., 1987, 1990); however, there are discrepancies in the precise role of HS and CS in this process. The discrepancies range from measurements of the GAG composition of the kidney to the effects of CS and HS on branching morphogenesis and mesenchymal to epithelial transformation. Compounding the confusion is the fact that all these studies were done in whole kidney organ culture, making it impossible to determine whether the effects on the UB are direct or indirect (via MM signals).

In this paper, we attempt to clarify the functions of HS and CS in UB branching morphogenesis using in vitro culture of the isolated UB. Our results indicate that while CS is the most abundant GAG within the developing kidney, HS appears to play a more significant role in modulating UB branching. We find that, in aggregate, sulfated GAGs regulate proliferation more than the branching pattern of the UB, likely through an HS-mediated effect. These findings put previous work on the role of sulfated proteoglycans in ureteric bud branching morphogenesis in perspective. We present a model of how HS regulates various stages of UB branching, from UB outgrowth to the cessation of UB branching, by modulating a growth-factor-dependent switch mechanism important in the transitioning from one stage of the branching program to another.

Materials and methods

Materials

Tissue culture media were obtained from Mediatech and bovine fetal calf serum obtained from Biowhittaker (East Rutherford, NJ). Transwell filters (0.4-μm pore size) were obtained from Costar (Corning, NY). Growth factor reduced

Matrigel and rat type I collagen were obtained from Becton Dickinson (Franklin Lakes, NJ). FGF1 and GDNF were obtained from R&D systems (Minneapolis, MN). FITC-conjugated *Dolichos bifloris* lectin (DB) was obtained from Vector Laboratories (Burlingame, CA). The primary antibodies against occludin [mouse monoclonal, Immunofluorescence (IF) 1:100] were from Zymed (San Francisco, CA); MT1-MMP (mouse monoclonal, IF: 1:500) and BrdU (mouse monoclonal, IF 1:100) was from Calbiochem (San Diego, CA); FGF-R2 (rabbit polyclonal, IF 1:100) from Santa Cruz (Santa Cruz, CA). Cy2, Cy3 antimouse, or antirabbit (IF: 1:100) secondary antibodies were from Jackson Immunoresearch Laboratories (West Grove, PA) as was Alexa-568 coupled phalloidin (IF: 1:100). Heparitinase (Heparin Lyase III) and chondroitinase ABC were obtained from Associates of Cape Cod (East Falmouth, MA). Decalin xyloside and naphthalene xyloside were synthesized as previously described (Lugemwa and Esko, 1991). Biotinylated FGF2 (IF: 1:500) was prepared as described (Bai et al., 2001). Plasticware was from Falcon (Lincoln Park, IL). All other reagents and chemicals, unless otherwise indicated, were from Sigma (St. Louis, MO).

DNA array analysis of proteoglycan expression patterns

RNA preparation and analysis of embryonic day13, e15, e17, e19, newborn, and adult rat kidneys was performed and data analyzed as previously described (Stuart et al., 2001). RNA from isolated UB from 0, 1, 3, and 5 days of culture and from metanephric mesenchyme induced by spinal cord at 0, 2, 4, 6, 14, 24, 72, and 120 h of culture was isolated using the Strataprep Total RNA Microprep kit (Stratagene, La Jolla, CA) as previously described (Stuart et al., 2003). Briefly, duplicate samples for each condition consisting of approximately 100 ng of total RNA were then used for reverse transcription (RT), second strand synthesis, and in vitro transcription (IVT) of cRNA. cRNA from the first round of IVT was recovered and used as a template in a second round of RT/IVT incorporating biotinylated nucleotides as per Affymetrix protocol, producing approximately 80 μg of labeled cRNA. Labeled cRNA probe (15 μg) was hybridized to Affymetrix Rat Genome U34A GeneChip (Affymetrix, Santa Clara, CA), washed, stained, and scanned per standard Affymetrix protocol. Data were analyzed as previously described (Qiao et al., 2001; Stuart et al., 2001), allowing assignment of statistical significance to observations and filtering for genes with the greatest relative changes in the context of their baseline expression. Double IVT expression data was compared with expression of the gene accession number of single IVT whole kidney mRNA expression.

[^{35}S] Sulfate labeling of glycosaminoglycans

Isolation of whole kidney rudiments was performed as described below. Isolated kidneys were cultured (37°C, 5% CO_2, 100% humidity) in DMEM media supplemented with 10% fetal calf serum and 100 μCi $^{35}SO_4$/ml and allowed to grow for 3–4 days. After exposure of the tissues to labeled precursors, medium was removed and samples were washed three times with PBS. Tissues were then processed as previously described (Esko et al., 1987).

Generation of BSN conditioned media

The Cellmax artificial capillary cell culture system was inoculated with BSN cells as previously described (Sakurai et al., 1997). Conditioned media was harvested according to the manufacturer's instructions.

Culture of isolated embryonic kidneys

Embryonic kidneys were isolated from gestational day 13.5 Sprague–Dawley rat embryos and applied to the top of Transwell filters placed within individual wells of a 12-well tissue culture dish. The isolated kidneys were cultured (37°C, 5% CO_2, 100% humidity) in DMEM/F12 media supplemented with 10% fetal calf serum and varying concentrations of sodium chlorate, heparitinase, chondroitinase ABC, and xylosides as indicated in the text. Kidneys were cultured for 3–4 days, then fixed in 4% paraformaldehyde and stained with fluorescein-conjugated *D. bifloris* lectin (1:100).

Isolation and culture of UB

UBs were separated from the MM of E13 rat kidneys as previously described (Qiao et al., 1999). Briefly, embryonic kidneys were lightly digested with trypsin and the UBs separated from the MM using fine-tipped needles. The UBs were suspended within a matrix containing growth factor-reduced Matrigel and Type I collagen (50:50 v/v) supplemented with DMEM and buffered by HEPES and $NaHCO_3$ to a pH of approximately 7.2. UBs were applied to the top of a Transwell filter and cultured in BSN-CM supplemented with 10% FCS, 125 ng/ml GDNF, and 375–500 ng/ml FGF1 and varying concentrations of sodium chlorate, heparitinase, chondroitinase ABC, decalin xyloside, and naphthalene xyloside as indicated in the text. UBs were allowed to grow for 6–7 days, then fixed in 4% paraformaldehyde and stained with fluorescein-conjugated *D. bifloris* lectin.

Immunocytochemistry and confocal analysis

Isolated UB grown in three-dimensional extracellular matrix gels or whole cultured kidneys were fixed in 4% paraformaldehyde (EM Sciences, Fort Washington, PA) for 30 min at room temperature and then washed with PBS. UBs were dissected from the Transwell insert and excess extracellular matrix (ECM) gel was removed. The UBs were equilibrated in quenching solution (20 mM glycine, 75 mM

NH_4Cl, 0.1% Triton X-100, in PBS without $Ca^{2+}Mg^{2+}$) for 30 min to reduce background fluorescence from the surrounding gel. Tissue samples were then incubated for 1 h at 4°C in blocking buffer [0.05% Triton X-100, 0.75% Fish gelatin (Sigma) in PBS]. Primary antibodies were diluted in blocking buffer and incubation was performed for 48 h at 4°C on a rocking stage. For control staining, primary antibody was omitted. After incubation, three washes with Solution I (0.05% Triton X-100 in PBS) were performed over 24 h at 4°C while rocking. Secondary antibodies in blocking buffer were incubated for 48 h at 4°C while rocking. Three washes in Solution I over a 24-h period at 4°C were then performed to remove unbound secondary antibody, and then the samples were mounted onto slides using Fluoromount (Southern Biotechnology Associated Inc, Birmingham, AL). Whole cultured kidneys were permeabilized in blocking buffer for 1 h at room temperature after fixation. Staining was then performed per the basic protocol as above. Fluorescence was examined by scanning laser confocal microscopy (Zeiss LSM-510). Images were processed with Photoshop software (Adobe, San Jose, CA).

Bromodeoxyuridine proliferation assay

Cultured whole kidneys were incubated for 3 h in the presence of 100 μM bromodeoxyuridine (BrdU) and cultured UBs were incubated for 12 h with 100 μM BrdU at 37°C. BrdU is incorporated into DNA of proliferating cells during the S-phase of the cell cycle. Extensive washes with PBS removed unincorporated BrdU. Whole kidneys and UBs were fixed in 4% paraformaldehyde for 30 min at room temperature (RT) and washed with PBS. Permeabilization with 0.075% Saponin for 30 min at RT followed by treatment with 1 N HCl for 30 min at RT were performed. Tissues were rinsed in PBS and the basic staining protocol was performed as described above. Samples were evaluated by scanning laser confocal microscopy.

TUNEL apoptosis assay

TUNEL labeling of DNA strand breaks was performed in whole kidneys and isolated UBs. Kidneys and isolated UBs were fixed in 1% paraformaldehyde for 30 min at RT and rinsed in PBS. The ECM gel was removed from around the isolated UBs. TUNEL staining was then performed according to the manufacturer's instructions (Intergen, Purchase, NY). Counterstaining with DB preceded mounting in Fluoromount. Samples were evaluated by scanning laser confocal microscopy.

Morphometric quantification

Whole embryonic kidneys were grown as described in the presence of sodium chlorate, heparitinase, chondroitinase ABC, and xylosides. Tissues were photographed at days 1, 3, and 5 then labeled with FITC-conjugated DB. Images were obtained with confocal microscopy. Geometric measurement of the DB-stained collecting system was obtained from at least four structures per day of interest using Image Pro Plus. These measurements include branch angle, stalk length and thickness, and total area. Angles are measured at branching points; stalk length is defined as the distance between branch points. Stick figures were generated as a composite of the average of these measurements. To account for differences in growth rate between control and treated kidneys, treated kidney stalk lengths were scaled to controls by normalizing with the ratio of the summed averages of control kidney stalk lengths to treated kidney stalk lengths.

Statistics

Each assay was performed in at least triplicate and data are presented as mean values ± SE The Student's t test was used to compare mean values between each experimental group. The ANOVA single factor test was applied to data from the morphometric quantification experiments. A P value of <0.05 was accepted to indicate statistical significance.

Results

Proteoglycans are differentially expressed during kidney development

We have previously analyzed the expression patterns of 8740 rat genes during whole kidney development and demonstrated global changes in gene expression (Stuart et al., 2001, 2003). This expression database was mined for specific PGs of interest to identify expression patterns. We first identified which PG sequences were represented on the Affymetrix rat U34A GeneChip by blasting known PG mRNA sequences against the oligonucleotide sequences synthesized on the GeneChip. Using techniques previously developed (Stuart et al., 2001, 2003), we then normalized expression data and represented expression as a function of maximal expression for each sequence. Additional information regarding the approach to data normalization is available at http://www.organogenesis.ucsd.edu.

Table 1 highlights PG core protein sequences (present on the U34A chip) that initially display the highest levels of relative expression during early rat kidney development and that then taper off during later fetal, neonatal, and adult periods. In whole kidney, this group included syndecan-1, glypican-1, glypican-2, and glypican-3 (all HSPGs), and versican (a CSPG). The highest levels of expression were during embryonic days 13 through 15, which correlate with initial UB branching and mesenchymal induction events. As discussed below, several of these PGs are particularly interesting in the context of renal development.

Table 1
Proteoglycans expressed during rat kidney development in vivo

Proteoglycan	Mutant phenotype	Fold difference (e13 to adult[a])
Falling transcript expression during kidney development		
Syndecan-1	Enhanced leukocyte adhesion to endothelia (Gotte et al., 2002) Transgenic has enhanced Wnt-dependent tumor formation (Alexander et al., 2000) Enhanced feeding behavior (Reizes et al., 2001)	5.2
Glypican-1	Unknown	5.3
Glypican-2	Unknown	9.6
Glypican-3	Nephromegaly, medullary dyplasia, hydroureter (Cano-Gauci et al., 1999)	16.1
Versican	Transgenic expression results in failure of endocardial cushion cell migration (Mjaatvedt et al., 1998)	16.9
Rising transcript expression during kidney development		
Agrin	Defective intramuscular nerve branching and presynaptic differentiation (Gautam et al., 1996)	1.5
Syndecan-2	Not reported	2.9
Syndecan-4	Mild defects in angiogenesis (Echtermeyer et al., 2001) and focal adhesion formation (Ishiguro et al., 2000) Increased susceptibility to renal damage (Ishiguro et al., 2001)	7.2
Biglycan	Reduced growth rate and decreased bone mass (Xu et al., 1998)	2.3
Decorin	Fragile skin (Danielson et al., 1997)	8.5

Proteoglycan core proteins listed are those that display developmentally regulated expression only in whole embryonic kidney. Core protein genes that were not represented on the gene chip include glypican-4, 5, and 6, syndecan-3 and collagen XVII.
[a] Gene expression analyzed in embryonic day13, e15, e17, e19, newborn, and adult rat kidneys (Stuart et al., 2001).

Table 1 also features those PG core proteins that exhibit highest levels of relative expression during late embryonic whole kidney development and in the neonate and adult. This group includes the HSPGs syndecan-2 and syndecan-4 and the CSPGs biglycan and decorin. Syndecan-4 knockout mice are found to have increased susceptibility to κ-carrageenan-induced obstructive nephropathy compared to wild type (Ishiguro et al., 2001); however, the roles for this group of PGs during renal development are unclear.

There were additional proteoglycan genes that did not display a developmentally regulated expression pattern. Our survey found that there was no significant change in expression of perlecan in the embryonic kidney. Perlecan knockout mice die at E10–12 due to ruptured basement membranes in the heart, although there are no renal abnormalities in the embryos that survive (Arikawa-Hirasawa et al., 1999; Costell et al., 1999). This analysis is limited by the representation of PGs on the GeneChip. For example, the uronic acid sulfotransferase, *Hs2st*, was not present on the gene chip we used, although there does appear to be a critical role for *Hs2st* in renal development (Bullock et al., 1998).

Using the whole kidney developmental data as a filter, we further investigated PG mRNA expression patterns in UB, MM, cultured isolated ureteric bud, and spinal-cord-induced metanephric mesenchyme and compared it to that of the whole embryonic kidney. This allowed us to determine if developmental regulation of these PGs was limited to the isolated UB or MM morphogenesis. It should be noted, however, that each tissue represents a separate experiment so that the absolute level between MM, UB, and WEK are not directly comparable. Our data indicate that there are marked changes in syndecan-4 and syndecan-1 expression in the epithelial ureteric bud during branching morphogenesis (Figs. 1A,B). Expression of these genes in the mesenchyme also appears to be regulated during nephrogenesis. Immunocytochemical studies have previously shown that syndecan-1 is transiently expressed in the metanephric mesenchyme and then assembles into the epithelium of the arborizing ureteric bud (Vainio et al., 1992). Versican, a CSPG that has been found to be essential in cardiac development, is also developmentally regulated in the isolated UB and MM (Fig. 1C). Expression of glypican-3 appears to be regulated in the isolated UB but not as significantly in the MM (Fig. 1D). On the other hand, the CSPG decorin is highly regulated in MM but not in the isolated UB (Fig. 1E). This in vitro expression data hints at more dynamic HSPG changes in the developing UB and more dynamic CSPG changes in the developing MM.

This approach has several limitations. Isolated culture of the UB may induce mRNA expression differently as compared to whole kidney culture when the UB is in intimate contact with mesenchyme; also, induction of MM with spinal cord may not be directly comparable to induction by the UB as spinal cord is a very potent inducer of mesenchymal differentiation, and it may be contributing an unknown factor for PG expression. However, the expression of both HSPG and CSPG core proteins are clearly regulated during kidney organogenesis, and the expression patterns detailed above are consistent with the concept that there may be some PGs primarily involved in ureteric bud branching while others may be specifically involved in mesenchymal induction.

Chondroitin sulfates are the predominant GAG synthesized by the developing kidney

The synthesis of HS and CS chains are also developmentally controlled. Studies performed over the last 20 years, however, have reported conflicting results regarding the relative contributions of CS and HS synthesis in the developing kidney (Lelongt et al., 1988; Platt et al., 1987). Our data support the finding that CS is the predominant sulfated glycosaminoglycan synthesized by the fetal kidney. By adding radioactive sulfate to the media of ex vivo cultured embryonic day 13 rat kidneys, all newly made GAGs were radiolabeled. After culture for 3 days, we then isolated the total GAGs from these kidneys and quantitated

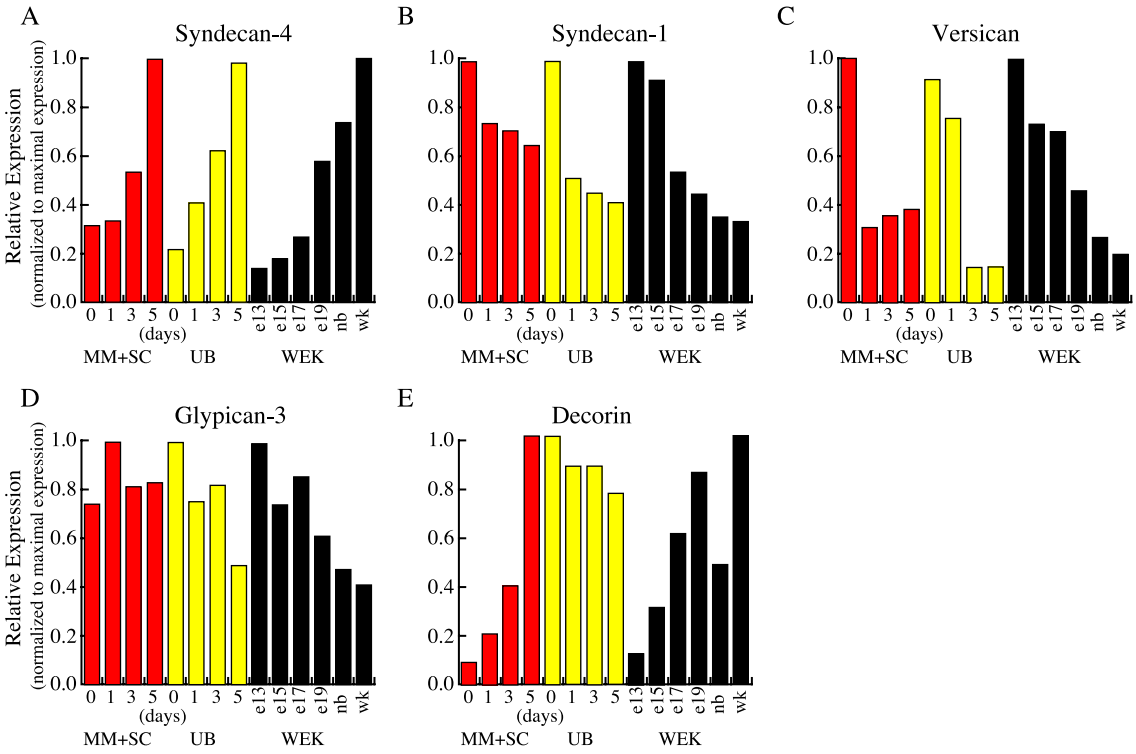

Fig. 1. Gene expression patterns in metanephric mesenchyme (MM) and isolated ureteric bud (iUB) and whole embryonic kidney (WEK). MM induced with spinal cord was cultured up to 5 days. Isolated UBs were cultured up to 5 days. WEK were isolated from embryos at various developmental stages as indicated. Using high-density DNA arrays, together with double in vitro transcription, gene expression patterns of specific proteoglycans (PG) of interest were analyzed in WEK, MM, and iUB as previously described (Qiao et al., 2001; Stuart et al., 2001, 2003), allowing assignment of statistical significance to observations and filtering of genes with the greatest relative changes in the context of their baseline expression. Graphs display representative time points for MM, iUB, and WEK PG gene expression normalized to maximal expression in each tissue, thus the levels of expression between MM, iUB, and WEK are not directly comparable. In some cases, the point with maximal expression is not shown. Syndecan-4 (A), syndecan-1 (B), and versican (C) are developmentally regulated during kidney organogenesis in both UB and MM. Glypican-3 (D) is regulated during UB branching but not nephrogenesis. Decorin (E) is highly regulated during nephrogenesis. WEK—whole embryonic kidney; nb—newborn; wk—1 week.

the incorporated sulfate (see Materials and methods). By digesting the isolated GAGs with chondroitinase ABC, we were then able to determine the ratio of HS and CS that comprised the total GAG concentration. We established that CS comprise approximately 77% of the total GAG population (and HS 23%) in the early embryonic rat kidney (Fig. 2). This result is similar to that reported in induced murine metanephric mesenchyme (Lash et al., 1983); thus, our findings may reflect that the majority of GAG synthesis occurring in the embryonic kidney arises from mesenchyme undergoing epithelial transformation and the contribution of UB GAG synthesis may be comparatively minor.

Perturbation of HS in embryonic kidney culture inhibits UB branching morphogenesis

Given the expression patterns of HSPGs and CSPGs and the predominance of CS synthesis, we sought to determine the specific roles that either CSPGs or HSPGs may play during early metanephric development by perturbing their function in whole rat embryonic kidney and in the isolated ureteric bud. Normal sulfation patterns were disrupted by adding exogenous sodium chlorate to the culture medium. Chlorate competitively blocks the formation of phophoadenosine 5′ -phosphosulfate, the sulfate donor utilized by the sulfotransferase enzymes that mediate polysaccharide sulfation, thus inhibiting sulfation of the newly made GAG chains (Greve et al., 1988; Humphries and Silbert, 1988). Existing PGs were also stripped of their GAG chains by the addition of either heparitinase or chondroitinase ABC to the culture medium. Finally, GAG synthesis on PG core proteins was diminished by the addition of exogenous xylosides, which act as a metabolic decoy for GAG synthesis (Schwartz et al., 1974). Naphthalene xyloside blocks the attachment of both HS and CS chains, whereas decalin xyloside only affects CS attachment (Fritz et al., 1994). It is worth noting that the action of perturbation by each of these compounds is different. In the case of chlorate, the sulfation of the GAG chain is inhibited, but the chain itself remains intact. With the glycolytic enzymes, heparitinase and chondroitinase ABC, the chains are degraded into biologically fragments. Xylosides, on the other hand, generate free chains within the media and block the addition of the chains to the proteoglycans; the free chains may have biological

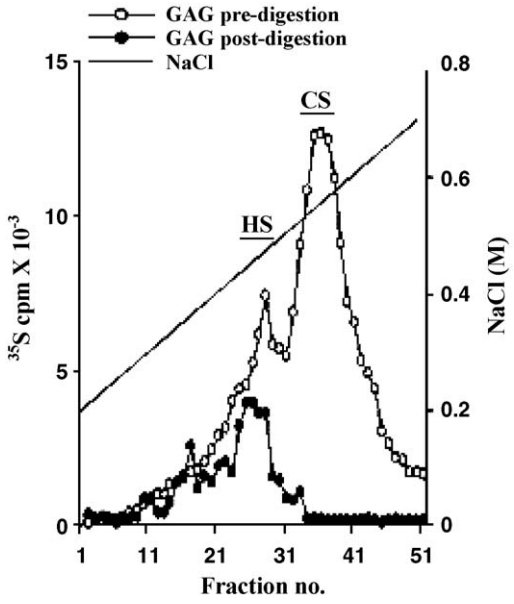

Fig. 2. Glycosaminoglycan (GAG) synthesis in cultured embryonic kidney. Newly synthesized ^{35}S-labeled GAGs were isolated from cultured embryonic day 13 rat kidneys. Elution of heparan sulfate (HS) and chondroitin sulfate (CS) was performed via HPLC. HS elutes earlier than CS. Before digestion with chondroitinase ABC (open circles), CS peak encompasses 77% of total labeled GAG isolated, and HS 23%. Digestion with chondroitinase ABC results in loss of the peak (closed circles), confirming the presence of CS.

properties as well, but their concentration is quite low so that the primary effect is generally felt to be due to the inhibition of GAG chain addition to core proteins.

Fig. 3 demonstrates functional GAG perturbation in rat embryonic kidney culture. Previous studies have used chlorate, heparitinase, and chondroitinase ABC to show that, in ex vivo mouse whole kidney culture, altering GAGs inhibited ureteric bud growth and branching but did not affect nephron development (Davies et al., 1995). The set of experiments shown in Fig. 3 extends this finding. Figs. 3A–J demonstrate immunofluorescence of representative images of rat whole embryonic kidneys subjected to various GAG perturbations that have been stained with FITC-labeled *D. bifloris* (DB) lectin, which specifically binds a carbohydrate antigen found on UB epithelia (Laitinen et al., 1987). Fig. 3K quantitates these findings and shows the number of ureteric bud tips per kidney, which can be considered a direct measurement of the extent of branching morphogenesis (Bush et al., 2004). UB branching was found to be inhibited in a dose dependent manner by chlorate (Figs. 3B–D). When chlorate treated kidneys were cultured with an excess of sulfate, which reverses the effect of chlorate, there was partial recovery of branching (Fig. 3E); more complete recovery of branching may have been inhibited due to the higher osmolarity of the media (due to excess sulfate). Treatment of whole embryonic kidney with heparitinase (Fig. 3F), but not chondroitinase (Fig. 3G), also markedly impairs branching of the UB. Inactivation of these enzymes by boiling resulted in restoration of branching to near normal levels (Fig. 3H). Finally, perturbation solely of CS synthesis using decalin xyloside only slightly affected branching of the UB (Fig. 3J) whereas perturbation of both CS and HS by using naphthalene xyloside significantly affected branching (Fig. 3I).

Unfortunately, there is no available xyloside that inhibits HS synthesis alone, but these data suggest that HS plays a substantially greater role in UB branching morphogenesis relative to CS. We also noted that heparitinase treated kidneys had nearly absent in vitro nephron formation (Fig. 3N), although this may due to an effect of impaired induction by the abnormally branched UB. On the other hand, treatment with chlorate or chondroitinase ABC did not appear to impair nephrogenesis (Figs. 3M,O). These findings stand in contrast to the aforementioned study (Davies et al., 1995), which suggests that perturbation of both HS and CS have roughly comparable effects on morphogenesis and growth of the ureteric bud in whole kidney culture; however, in the previous studies, the authors may not have been able to determine specific effects on the UB owing to the lack of a suitable assay, which has recently been developed (Qiao et al., 1999) (see below).

Perturbation of HS in isolated UB culture inhibits normal branching morphogenesis

While these results confirm that HSPGs are important mediators of branching morphogenesis in the whole embryonic rat kidney, they do not allow independent examination of ureteric development isolated from local mesenchymal factors. That is, when utilizing the whole kidney culture model of renal development, "primary" effects on the ureteric bud cannot be separated from effects mediated by the local mesenchyme. This is a limitation of prior studies (Davies et al., 1995; Lelongt et al., 1988; Platt et al., 1990). Selective perturbation experiments were therefore carried out on isolated ureteric bud culture where UBs isolated from embryonic day 13 kidney rudiments are suspended within a three-dimensional extracellular matrix and cultured in a metanephric mesenchyme cell line conditioned media supplemented with GDNF and FGF1 (Qiao et al., 1999, 2001). Fig. 4 shows the addition of chlorate to the isolated ureteric bud culture. Both overall size and extent of branching are affected by perturbation of sulfation (Figs. 4B,D). The dose dependent effect (Fig. 4A) was rescued by addition of sulfate (Fig. 4D). Fig. 5 demonstrates representative images of isolated UBs treated with chondroitinase ABC (Figs. 5B,C) and heparitinase (Figs. 5D–F). These studies confirm that the decrease in branching and size of the bud is a dose-dependent function of perturbation of HS (Fig. 5H) but not CS activity (Fig. 5G). Finally, naphthalene xyloside and decalin xyloside were added to isolated UB culture. Naphthalene xyloside, which perturbs both HS and CS attachment to PG core proteins, decreased UB branching by approximately 50% (Figs. 6A–D,I). Decalin xyloside, which interferes only with CS attachment, decreased UB

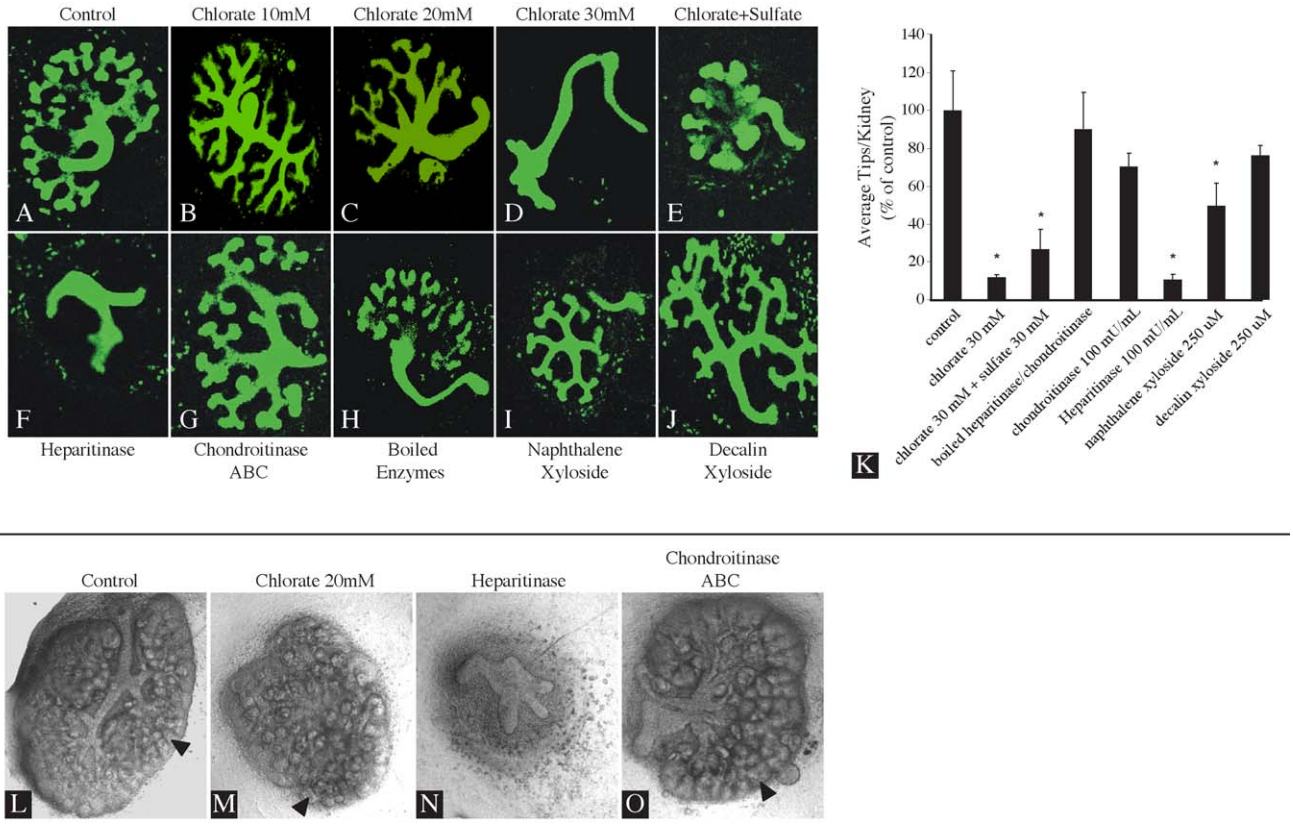

Fig. 3. Effects of perturbation of heparan sulfate (HS) and chondroitin sulfate (CS) in cultured embryonic kidney. (A–J) Embryonic day 13 rat kidneys were isolated and cultured in vitro for 3 days, then labeled with FITC-conjugated *D. bifloris* lectin. Kidneys were grown in the absence (A, control) or presence of varying concentrations of sodium chlorate (B–D), sodium chlorate (30 mM) plus sulfate (30 mM) (E), heparitinase (F, 100 mU/ml), chondroitinase ABC (G, 100 mU/ml), boiled heparitinase, and chondroitinase ABC (H), naphthalene xyloside that inhibits native synthesis of both HS and CS (I, 250 μM), or decalin xyloside that inhibits native synthesis of CS alone (J, 250 μM). Far right panel (K): Graphical analysis of the average number of tips per kidney as a percentage of control in whole kidney cultured with 30 mM chlorate (D), chlorate plus sulfate (E), boiled heparitinase and chondroitinase ABC (H), chondroitinase ABC (G), heparitinase (F), naphthalene xyloside (I), or decalin xyloside (J). Mean ± SEM, $n \geq 3$, $^*P \leq 0.05$ (compared to control). (L–O) Phase-contrast images of whole embryonic kidneys cultured in vitro for 4–5 days in the absence (L, control) or presence of 20 mM sodium chlorate (M), 100 mU/ml heparitinase (N), or 100 mU/ml chondroitinase ABC (O). Arrowheads indicate areas of mesenchymal to epithelial transformation (nephrogenesis); note the absence of the characteristic swirls of mesenchymal to epithelial transformation in heparitinase-treated kidneys.

branching by approximately 25%, a result that was not statistically significant (Figs. 6E–H,J). These results indicate that perturbation of endogenous HS function significantly interferes with primary ureteric bud branching, both in whole embryonic kidney culture and in isolated ureteric bud culture. The role of CS in UB branching appears to be considerably less than HS. It is possible that CS is involved in branching morphogenesis on a more subtle level compared to HS; however, the methods of quantitation used in this study likely lack the sensitivity to detect such effects.

To further support the idea that the morphological changes of the UB seen with GAG perturbation is actually due to diminished HS function, we evaluated the binding of FGF2 to whole kidneys and isolated UBs treated with chlorate. A well-defined function of HS is to facilitate binding of growth factors to their high-affinity receptors (Krufka et al., 1996). This interaction is often determined by the sulfation pattern of the HS molecule and has been best characterized in several cell culture models of FGF2-mediated receptor activation (Nakato and Kimata, 2002); thus, assessment of FGF2 binding is an indirect means of evaluating HS sulfation. Under control conditions (Figs. 7A,B), FGF2 is found to be bound throughout the developing nephrons (on both the ureteric bud and mesenchyme derived segments). In the presence of chlorate, FGF2 binding is markedly diminished (Figs. 7C,D). Diminution in FGF2 binding also occurred in isolated UBs cultured with chlorate. Figs. 7E and F show the isolated UB grown under control conditions and Figs. 7G and H in the presence of chlorate. Note that FGF2 binding is wholly confined to the basement membrane. There also appears to be a predominance of binding in the stalk regions vs. the ampullae of chlorate treated isolated UBs, which may represent differential binding of FGF2 along the arborizing UB.

Perturbation of HSPGs and CSPGs does not significantly change branch angles and stalk lengths of the UB

The inhibitory effects of nonselective HS perturbation on UB branching morphogenesis could either be a result of a

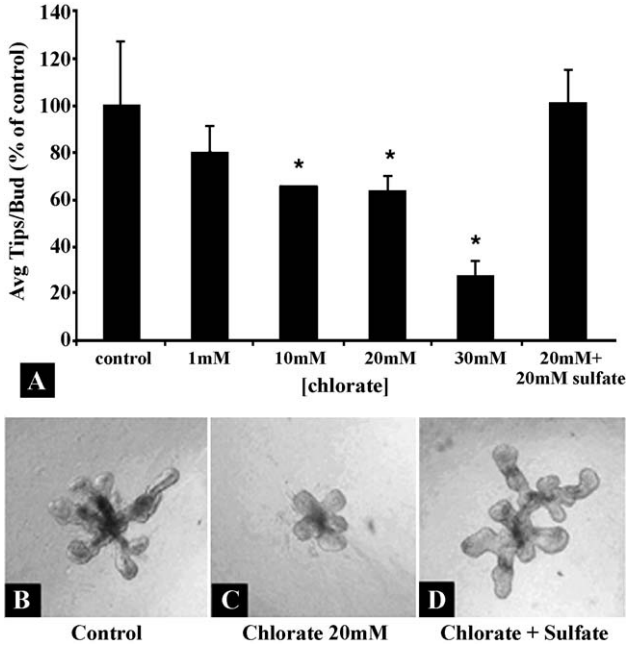

Fig. 4. Effects of chlorate on branching of isolated ureteric bud (iUB). Graphical analysis of the average number of tips (compared to control) per isolated rat UB cultured in vitro for 6–7 days with varying concentrations of sodium chlorate (1, 10, 20, and 30 mM) and sodium chlorate 20 mM + sulfate 20 mM (A). Mean ± SEM, $n \geq 3$, $^*P \leq 0.05$ (compared to control). Bottom panel (B–D) displays representative phase-contrast photomicrographs of iUBs cultured in the absence (B, control) or presence of 20 mM chlorate (C), and chlorate (20 mM) plus sulfate (20 mM) (D).

change in the growth rate or in the arborization pattern (e.g., fewer branching events or reorganization of the spatial branching arrangement). We therefore quantified the reduction in the number of branch tips in kidneys exposed to chlorate, heparitinase, or chondroitinase ABC by evaluating whole kidney area and branch angles and stalk lengths at each iteration of branching in control and in GAG-perturbed kidneys. This analysis allows for relatively independent evaluation of growth (based on tip number and area) and branching pattern (based on relative stalk length and branch angle) (Bush et al., 2004). Under control conditions, branching occurs in a uniform manner with fairly consistent stalk lengths and branch angles. The result is a highly ordered, arborized structure that maximizes area and minimizes internal contacts. Fig. 8A shows the average area of control, chlorate-, chondroitinase-, and heparitinase-treated kidneys. Chlorate at higher concentrations (20 and 30 mM) and heparitinase cause a significant reduction in the area of the kidney, while lower concentrations of chlorate (10 mM) and chondroitinase ABC treatment are similar to control. In contrast, the average branch angle and stalk length did not differ significantly between control and GAG perturbed kidneys at the first branching iteration (Fig. 8B). The second branching iteration also does not display significant differences between control and treated kidneys although heparitinase-treated kidneys tend to have greater variations in branch length compared to the other conditions (Fig. 8C). Fig. 8D shows computer-generated composite models of

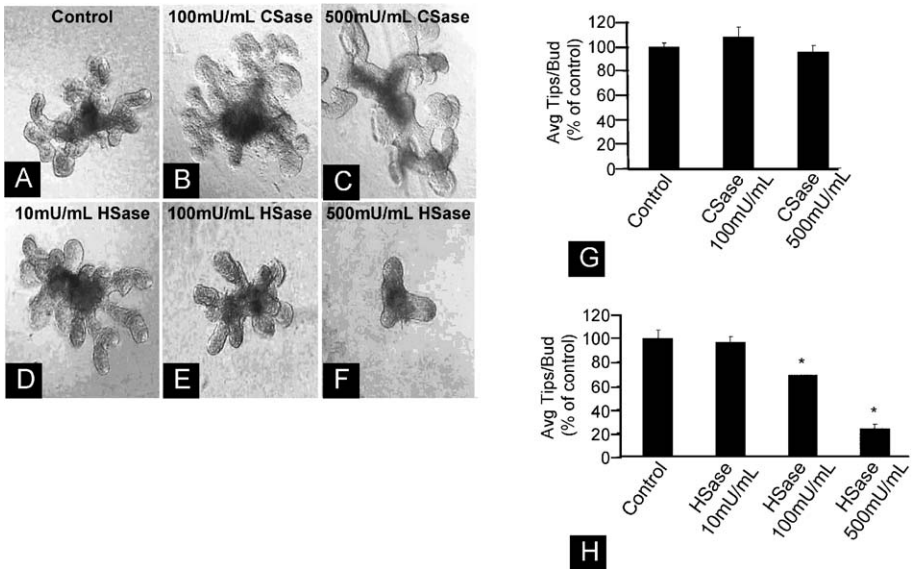

Fig. 5. Effects of chondroitinase ABC (CSase) and heparitinase (HSase) on branching of isolated ureteric bud (UB). (A–F) Representative phase-contrast photomicrographs of iUBs cultured in the absence (A, control) or presence of chondroitinase ABC 100 mU/ml (B), 500 mU/ml (C), or heparitinase 10 mU/ml (D), 100 mU/ml (E), 500 mU/ml (F). Far right top panel, (G): graphical analysis of the average number of tips (compared to control) per isolated rat UB cultured with chondroitinase ABC 100 mU/ml (B) and 500 mU/ml (C). Far right bottom panel (H): graphical analysis of the average number of tips (compared to control) per isolated rat UB cultured with heparitinase 10 mU/ml (D), 100 mU/ml (E), and 500 mU/ml (F). Mean ± SEM, $n \geq 3$, $^*P \leq 0.05$ (compared to control).

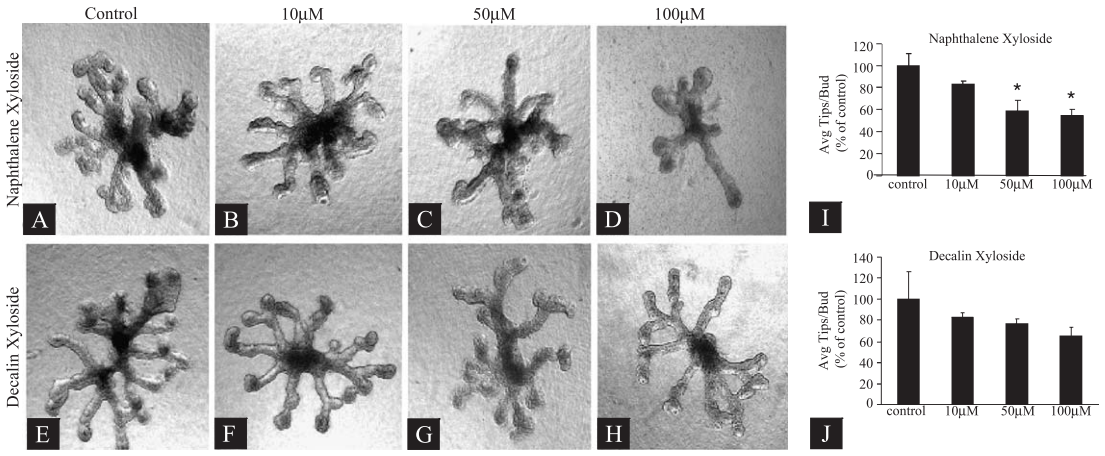

Fig. 6. Effects of naphthalene xyloside and decalin xyloside on branching of isolated ureteric bud (UB). (A–H) Representative phase-contrast photomicrographs of iUBs cultured in the absence (A, control) or presence of naphthalene xyloside 10 μM (B), 50 μM (C), 100 μM (D); or decalin xyloside 10 μM (F), 50 μM (G), 100 μM (H). Far right top panel, (I): graphical analysis of the average number of tips (compared to control) per isolated rat UB cultured with naphthalene xyloside 10 μM (B), 50 μM (C), 100 μM (D). Far right bottom panel (H): graphical analysis of the average number of tips (compared to control) per isolated rat UB cultured with decalin xyloside 10 μM (F), 50 μM (G), 100 μM (H). Mean ± SEM, $n \geq 3$, $^*P \leq 0.05$ (compared to control).

chlorate- and heparitinase-treated embryonic kidneys compared to control. These models were scaled to account for differences in growth rate as distinct from branching events. The superimposed figures demonstrate that chlorate-treated kidneys have essentially the same branching pattern as controls. On the other hand, despite similar branch lengths and angles (i.e., patterning), heparitinase-treated kidneys are stunted and appear markedly different from control. A similar phenotype is seen in kidneys treated with 30 mM chlorate (not shown). These results suggest that nonselective perturbation of HS disrupts normal "growth" signals within the developing UB and that CS perturbation does not affect these instructive signals. In these experiments, all types of heparan sulfation are presumed to be perturbed; selective perturbations (e.g., in O-sulfation or N-sulfation), which may affect signaling of a specific growth factor, may reveal patterning defects.

Proliferation is decreased in embryonic kidneys and isolated UBs with altered GAG sulfation

Given the above results, we further investigated the mechanism for the growth retardation observed after GAG perturbation by evaluating proliferation and apoptosis in

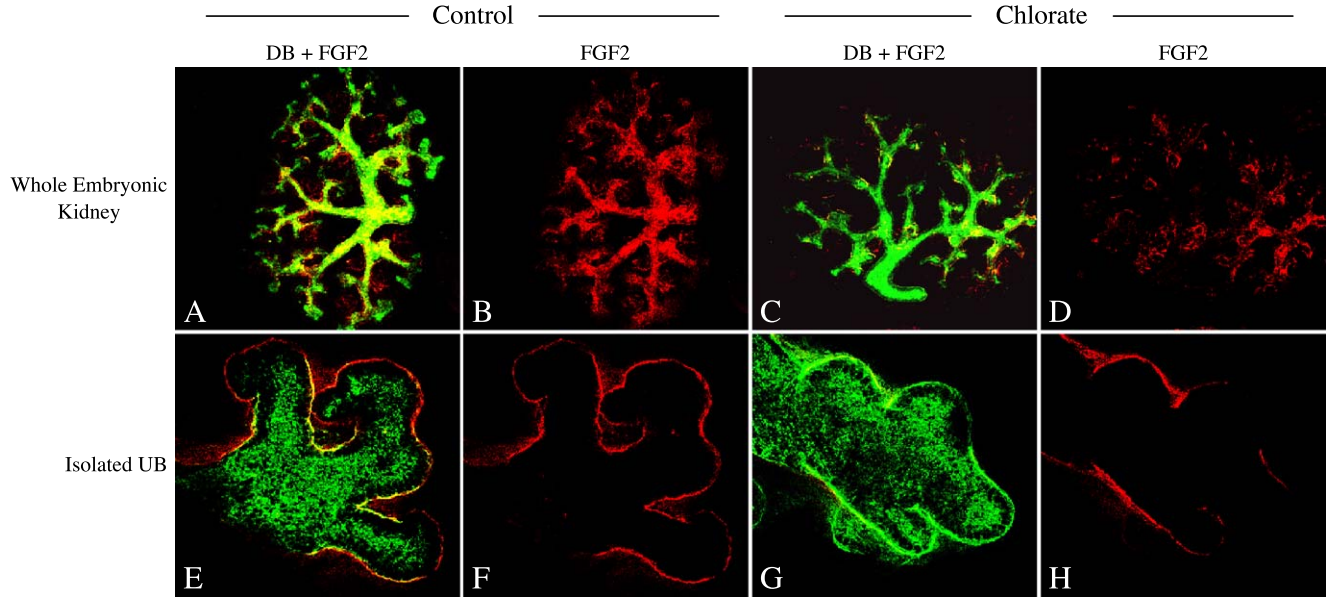

Fig. 7. FGF2 localization in cultured embryonic rat kidney and isolated rat ureteric bud (UB). Diminished FGF2 binding in chlorate-treated kidneys is demonstrated with immunofluorescent labeling of biotin-conjugated FGF2 (red) and *D. bifloris* (DB) (green). Immunocytochemistry was performed in embryonic day 13 kidney cultured in the absence (A,B control) or presence of chlorate 10 mM (C,D). FGF2 is found on both UB and mesenchymal structures while DB stains only UB. Bottom row (E–H) displays FGF2 staining of cultured isolated UB in the absence (E,F control) or presence of chlorate 30 mM (G,H).

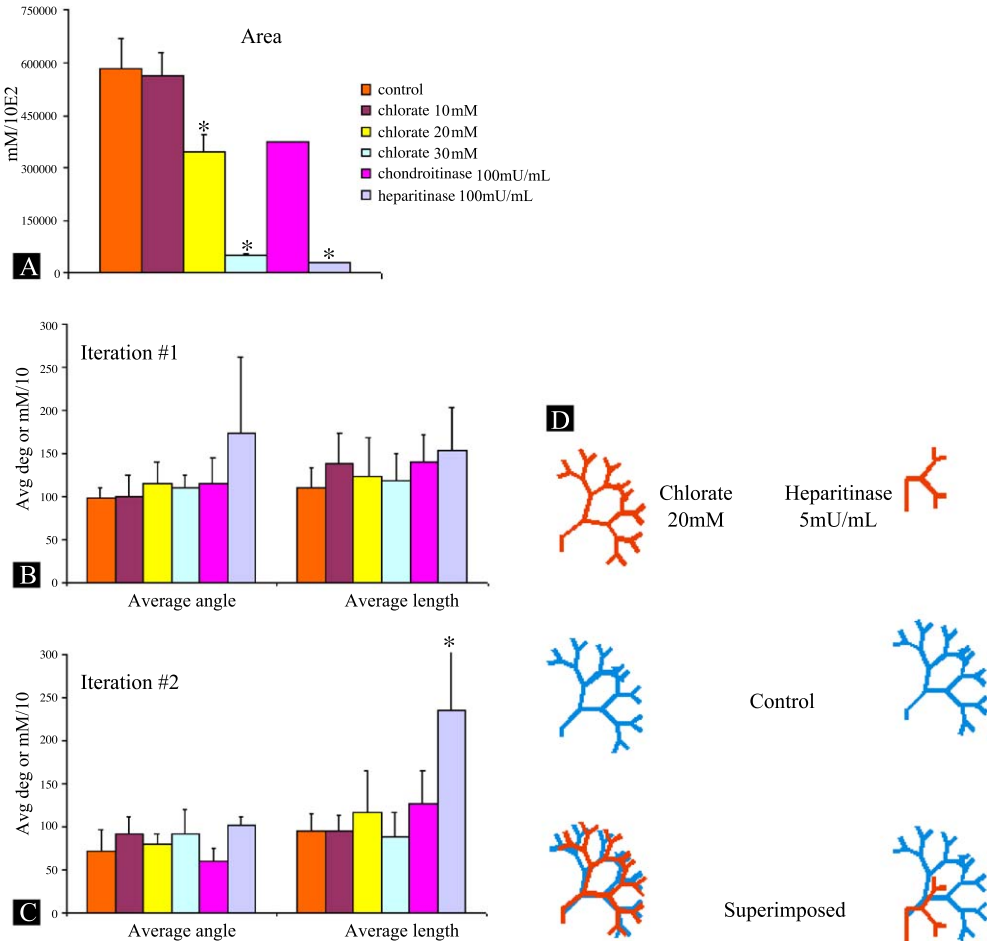

Fig. 8. Area, branch angles, and stalk lengths in embryonic rat kidney. Graphs depict average area (A), average branch angle, and length at the first iteration of branching (B), and the average branch angle and length at the second iteration of branching (C) in embryonic kidneys grown in the absence and presence of various glycosaminoglycan perturbations. Figure legend in panel A represents all panels. Mean ± SEM, $n \geq 3$, $^*P \leq 0.05$ (compared to control). (D) Composite models of branching in embryonic rat kidney. Stick figures represent average branch angle and stalk length at each iteration of branching, normalized for differences in growth rate, in kidneys grown in the presence of chlorate 20 mM or heparitinase 5 mU/ml compared to control. Tip number is not represented in this analysis.

the cultured embryonic kidney and isolated UB. Relatively little is known about the balance of proliferation and apoptosis in creating branch tips and stalks. Prior studies in murine kidney rudiments have shown that the highest rates of proliferation occur in uninduced mesenchyme, the early stages of epithelial differentiation, and the tips of the collecting ducts (Mugrauer and Ekblom, 1991), while apoptosis appears to be most prominent in uninduced mesenchyme (Koseki et al., 1992). Additionally, we have recently extended these findings to show that in the isolated ureteric bud, proliferation is almost wholly confined to the distal tips of the branches (ampullae) while apoptosis occurs at a higher rate in the branch stalks (Meyer et al., submitted for publication). Disruption in the balance of proliferation and apoptosis therefore likely alters growth and possibly normal arborization patterns. This is seen in cystic kidney disease where proliferation and apoptosis are both diffusely increased and lead to altered morphology and function of the tubules (Grisaru et al., 2001).

Proliferation was evaluated by in vitro BrdU incorporation and subsequent immunocytochemistry for BrdU. Similar to the aforementioned study, proliferating cells were found primarily in the ampullae of control kidneys (Fig. 9A). Chlorate-treated kidneys had a markedly diminished rate of proliferation although the localization remained the same (Fig. 9B). The same distribution of proliferation is found in the isolated UB (Figs. 9C,D). This result suggests that there is a putative molecule that stimulates ampullary growth that is bound by HS or CS and its binding or function (or both) is dependent on proper sulfation of the GAG. Figs. 9E and F show apoptosis detected by TUNEL staining of 3′ DNA fragmentation in control and chlorate-treated isolated UBs. Apoptotic cells were primarily found in the stalks in both isolated UBs grown under control conditions (Fig. 9E) and those in the presence of chlorate (Fig. 9F).

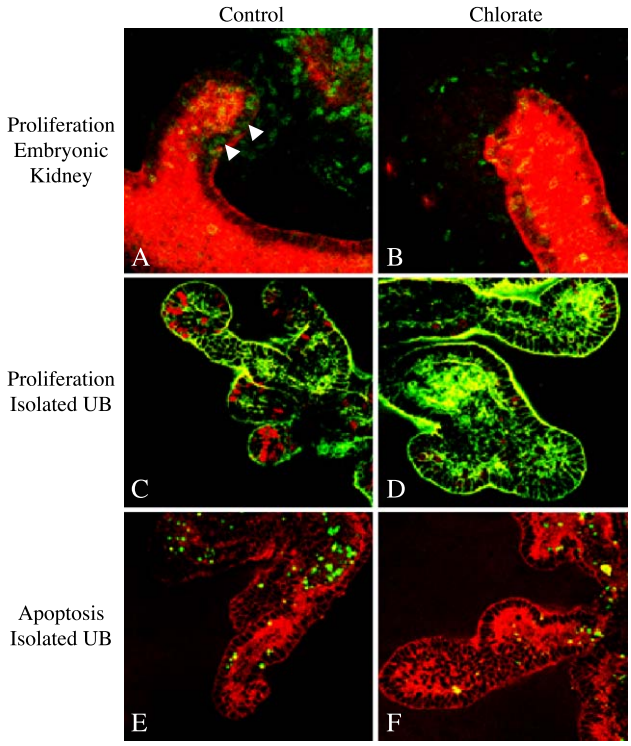

Fig. 9. Proliferation and apoptosis in cultured rat embryonic kidney and isolated ureteric bud (UB). (A,B) Confocal microscopic immunofluorescent localization of BrdU (green) in day 13 embryonic kidneys cultured in the absence (A, control) or presence of chlorate 30 mM (B) for 3 days (*D. bifloris* staining in red). As described in controls, proliferation appears to be localized to the UB ampullae (A, arrowheads) and adjacent mesenchyme. (C,D) Localization of BrdU (red) in isolated UB cultured without (C, control) and with chlorate 30 mM (D) for 7 days (*D. bifloris* staining in green). TUNEL staining (green) was performed on isolated UBs in the absence (E, control) or presence of chlorate 30 mM (F). *D. bifloris* staining appears in red. Apoptosis occurs primarily in stalks of the UB as described.

FGFR2 and epithelial markers are unchanged by GAG perturbation

Given that proliferation is diminished when GAGs are perturbed and that FGF2 binding is affected by HS perturbation, we also examined the localization of FGFR2, another member of the FGF2 signaling complex. FGFR2 is found in collecting ducts and some nephron tubules in the developing kidney and is thought to be involved in the induction of UB outgrowth and the mesenchymal–epithelial conversion (Cancilla et al., 1999; Qiao et al., 2001). Fig. 10 displays immunofluorescence of FGFR2 on the isolated UB. Under control conditions (Fig. 10A), FGFR2 was found predominantly on the basolateral surfaces of the epithelial cells that make up the UB, which is the surface exposed to the extracellular matrix, and there appears to be a predominance of expression at the tip of the UB branch. When the isolated UB is cultured in media containing various GAG-perturbing compounds, we found that FGFR2 localization was unchanged, at least at the level of immunocytochemistry (Figs. 10B–D). This then suggests that FGFR2 localization and expression is independent of GAG function.

Next, we investigated if the change in morphology of isolated UBs with altered GAGs was secondary to changes in effector molecule localization or expression. We first examined junctional proteins that delineate apical and basal surfaces of the tubular epithelium, β-catenin, an adherens junction protein, and occludin, a tight junction protein. The spatial localization of these proteins appears qualitatively unaffected by treatment with chlorate (Figs. 11D,E), heparitinase (Figs. 11G,H), or chondroitinase (data not shown). We also found that the localization of another key effector of branching morphogenesis, MT1-MMP, a membrane-bound metalloproteinase involved in matrix degradation of developing epithelial structures that has been found to regulate UB branching morphogenesis (Pohl et al., 2000a), was also unaffected by GAG perturbation with chlorate or heparitinase as determined by immunocytochemistry (Figs. 11F,I). As these molecules are thought to be important in UB patterning, these results seem to be generally consistent *with a defect in overall growth rather than patterning after non selective HS perturbation*.

Discussion

The goal of the present study was to delineate the role of heparan sulfate proteoglycans (HSPG) and chondroitin sul-

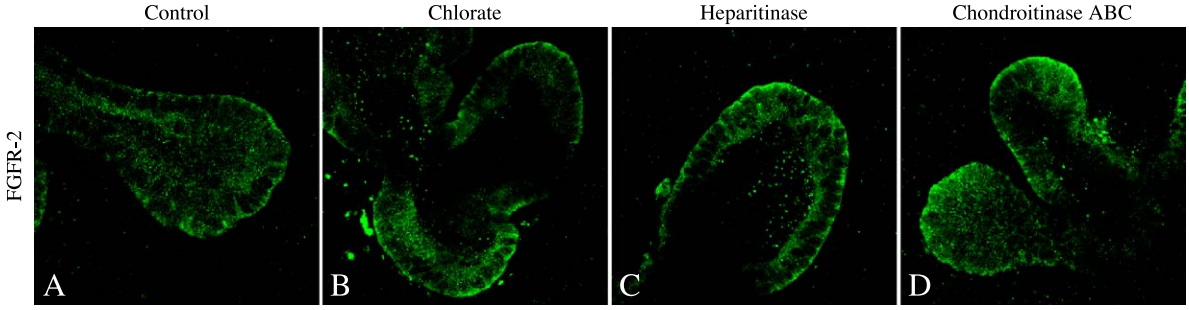

Fig. 10. Localization of FGFR-2 in cultured isolated rat ureteric bud (UB). Isolated UBs grown for 7 days in culture were stained for FGFR-2 in the absence (A, control) or presence of chlorate 30 mM (B), heparitinase 100 mU/ml (C), or chondroitinase ABC 100 mU/ml (D).

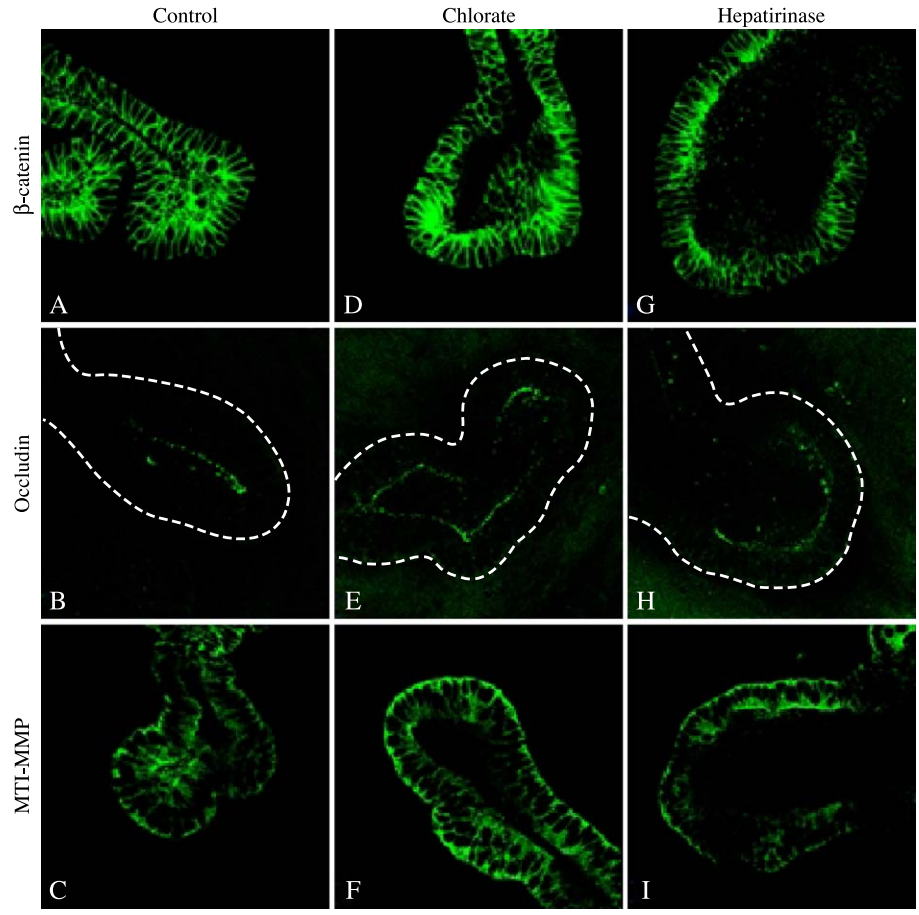

Fig. 11. Localization of effector molecules in cultured isolated rat ureteric bud (UB). Isolated UBs grown for 7 days in culture were stained for the adherens junction protein, β-catenin (A, D, G), the tight junction protein, occludin (B, E, H), and the matrix metalloproteinase, MT1-MMP (C, F, I), in the absence (A, B, C, control) or presence of chlorate 30 mM (D, E, F) or heparitinase 100 mU/ml (G, H, I). Occludin (B, E, H) is found on the apical surfaces of UB cells, the outline of the UB is marked with the dashed line.

fate proteoglycans (CSPG) in ureteric bud branching morphogenesis. The difference with previous, sometimes conflicting studies, done in whole embryonic kidney about a decade ago (Davies et al., 1995; Lelongt et al., 1988; Platt et al., 1990) is that we have directly examined ureteric bud (UB) branching in the recently developed isolated UB culture system and placed these findings in the context of parallel experiments done with the whole embryonic kidney in organ culture. Furthermore, we have supplemented the studies with microarray data in several pertinent in vitro model systems.

Branching morphogenesis in cell culture is known to be greatly influenced by extracellular matrix composition (Santos and Nigam, 1993). In this report, we show that HSPGs play a prominent role in the process of UB branching morphogenesis while CSPGs appear less critically involved. Some of our data are consistent with previously published results that demonstrate that disruption of proteoglycans dramatically alters epithelial organogenesis of the kidney (Davies et al., 1995; Platt et al., 1987). Our results show that undersulfation of both HS and CS with chlorate causes a reduction in the number of ureteric bud tips presumably due to a primary effect of HS undersulfation since specific degradation of CS chains with chondoitinase ABC does not significantly affect UB branching. Using an in vitro isolated UB culture assay, we found that the branching abnormalities noted with HS perturbation occur through a direct effect of HS upon the UB (rather than the potential effects of HS perturbation on mesenchymal induction of UB branching). This mechanism may account for the reduced number of UB branch tips seen in chlorate-treated kidneys; in addition, HS may also have an effect upon nascent MM-derived epithelial structures that ultimately form nephrons and help determine nephron number. These findings suggest that HS, presumably on the UB cell surface or within the UB basement membrane, can modulate branching morphogenesis in the developing kidney.

That perturbation of HS predominantly affects early UB growth and branching in this study suggests that there may be an HS "microenvironment" along the UB that modulates specific growth factor signaling as well as the generation of local and global gradients of stimulatory and inhibitory growth factors (Nigam, 1995; Santos and Nigam, 1993; Stuart et al., 1995). The generation of a local microenvironment of GAG chains relies upon the strictly controlled

spatial and temporal presentation of HS and CS chains. Because the synthesis of GAGs is not regulated at the transcriptional level, spatiotemporal control must occur through other mechanisms. Protein cores may play an integral role in this regard. We found several protein core genes that were developmentally regulated in both the UB and MM including syndecan-1, syndecan-4, and versican. Regulation of expression of other genes appeared to be confined to the UB (glypican-1,2,3) or the MM (decorin) alone, suggesting that there may also be microenvironments within the MM that modulate developmental processes during kidney organogenesis. The precise role of the core proteins in development has not been well characterized, although knockout data support their function in UB branching morphogenesis. This is demonstrated in glypican-3-deficient mice that display a phenotype very similar to the human Simpson–Golabi–Behmel syndrome, characterized by renal cystic dysplasia (Pilia et al., 1996). In the human Simpson–Golabi–Behmel syndrome, affected individuals have a mutation in the glypican-3 gene.

Although the proteoglycan core proteins determine the spatial and temporal location of the HS chains, the HS biosynthetic enzymes ultimately determine HS fine structure. Environments of specifically sulfated HS chains may represent a subset of the overall HS microenvironment that eventually governs the growth-factor-mediated morphogenetic event. One fundamental mechanism by which HS facilitates growth factor signaling is to stabilize the growth factor and receptor complex to sustain signaling (reviewed in Ornitz, 2000). HS can also act as a coreceptor for growth factor signaling (reviewed in Tumova et al., 2000). These types of HS growth factor interactions have been well studied in FGF2 signaling (Pye et al., 1998; Rapraeger et al., 1991; Yayon et al., 1991). In UB branching morphogenesis, HS–growth factor–growth factor receptor complexes and their downstream signals likely determine the morphogenetic event that occurs in the developing epithelial structure (Nigam, 2003). We have previously reported that various stimulatory and inhibitory growth factors are able to "sculpt" the UB during morphogenesis (Bush et al., 2004; Qiao et al., 2001). In the setting of HS perturbation, one might expect that the binding or activity of fibroblast growth factors other than FGF2 is similarly disrupted so that the normal instructive signals that govern the patterning and growth of the kidney are interrupted.

Another function of HSPGs may be to create a "sink" of growth factors or other signaling molecules that can be released in a time- and gradient-dependent fashion. The substantial decrease in labeled FGF2 binding seen whole embryonic kidney and isolated UB after treatment with chlorate supports this notion. Furthermore, the release of FGF2 from the basement membrane HSPG, perlecan occurs via matrix metalloproteinases that degrade the protein component of the proteoglycan (Whitelock et al., 1996). HS also binds MMPs and may provide a reservoir of MMPs within the extracellular space (Yu and Woessner, 2000). Matrix metalloproteinases have been shown to be modulators of UB branching morphogenesis in vitro (Pohl et al., 2000a), and their activity is attenuated by heparin and heparan sulfate (Yu and Woessner, 2000). In this study, the localization of MT1-MMP in the branching UB was not qualitatively altered by GAG perturbation although its activity, which was not measured in this study, may be changed in this setting.

It is becoming evident that HS fine sulfation pattern plays a significant role in many of the growth factor mediated morphogenetic events that are required for branching morphogenesis, from modulation of growth factor signaling to gradient formation (Nigam, 1995; Santos and Nigam, 1993; Stuart et al., 1995). There is now data to suggest that 2-O- and 6-O-sulfated HS are involved in different aspects of growth factor signaling (reviewed in Faham et al., 1998; Lyon and Gallagher, 1998). Cell culture models have shown that chlorate treatment of Madin–Darby canine kidney cells results in differential effects upon 6-O-sulfation vs. 2-O-sulfation (Safaiyan et al., 1999). In this model, low chlorate concentrations (5–20 mM chlorate) selectively reduced the 6-O-sulfation of HS, whereas treatment with higher concentrations of chlorate (50 mM) reduced both 2-O- and 6-O-sulfation. In our experiments with high concentrations of chlorate, we may be inhibiting both 6-O-sulfation and 2-O-sulfation, and thus approximating a milieu that is similar to the 2-O-sulfotransferase knockout in which there is failure of ureteric bud branching. Heparan sulfate has been reported to be required for GDNF signaling (Barnett et al., 2002), and a recent study has shown that the bioactivity of GDNF may be dependent on binding to 2-O-sulfate-rich, heparin-related glycosaminoglycans (Rickard et al., 2003). Interestingly, GDNF knockout mice also have renal agenesis (Sanchez et al., 1996); thus the phenotype we observe with high dose chlorate may, in part, be due to impairment of GDNF signaling that is mediated by 2-O-sulfated HS. Kidneys treated with lower concentrations of chlorate, which may be selectively affecting 6-O-sulfation, have reduced branch tip numbers without appreciable differences in branching pattern. These findings could have clinical relevance as it may be that alterations in nephron number, which are postulated to lead to the development of hypertension (Brenner et al., 1988), and may in some cases be due to a proteoglycan-related aberration (Shah et al., 2004).

Taken together, our findings begin to bring together the interaction between growth factors, growth factor receptors, and proteoglycans in the patterning and growth of the embryonic kidney. While others have suggested that both HSPGs and CSPGs are necessary for ureteric bud branching, we find that isolated UB branching is predominantly modulated by HSPGs. However, it is plausible that CSPGs also modulate branching but on a more subtle level; through more detailed morphometric quantification and gene expression analysis, the role of CSPGs on branching morphogenesis may become apparent.

Branching of the UB is an iterative process of branch point formation and stalk elongation that results in an

arborized structure. We have recently proposed a model in which UB branching proceeds through stages that are broadly characterized by (1) UB outgrowth from the Wolffian duct (prebranching); (2) a rapid branching and growth phase where "feedforward" mechanisms predominate; (3) a slowing down of branching regulated by feedback mechanisms; and (4) a stop branching/maturation process (Bush et al., 2004; Nigam, 2003). These stages can be distinguished by a unique combination/set of heparin-binding growth factors; for example, FGFs and pleiotrophin modulate rapid growth and branching (stage 1) (Qiao et al., 2001; Sakurai et al., 2001), while members of the TGFβ superfamily act to slow branching (stage 2) (Bush et al., 2004). Disruption of phase-specific molecular pathways may result in groups of syndromes that are phenotypically similar (Shah et al., 2004). For example, renal agenesis occurs when initial growth and branching signals are interrupted and cystic kidney disease tends to occur in the setting of improper stop signals. Based on this and other recent studies, we propose that these stages are pivotally regulated (both positively and negatively) by growth factor–sulfated proteoglycan interactions (Bush et al., 2004; Nigam, 2003; Stuart et al., 2003). In addition, although not discussed here, these morphogenetic stages may also be influenced by HSPG interactions with insoluble ECM ligands. Studies of syndecan-4-deficient fibroblasts show that these cells have a reduced rate of migration during in vitro wound healing perhaps due to altered fibronectin signaling of actin stress fiber assembly and focal adhesion (Echtermeyer et al., 2001). Similar mechanisms may be operative during invasion of the UB into the MM. This interplay among soluble and insoluble ligands bound by sulfated proteoglycans, matrix proteases capable of liberating bound ligands, and receptor tyrosine kinases, which depend on interactions with both their ligands and proteoglycans for activation, presumably set in motion the intracellular events that lead to the developmental processes involved in branching morphogenesis.

Based on our findings, we propose a model (Fig. 12) where microenvironments of HS, established through spatiotemporally controlled expression of protein cores and biosynthetic enzymes, modulate a variety of morphogenetic events from branch point formation to stalk elongation.

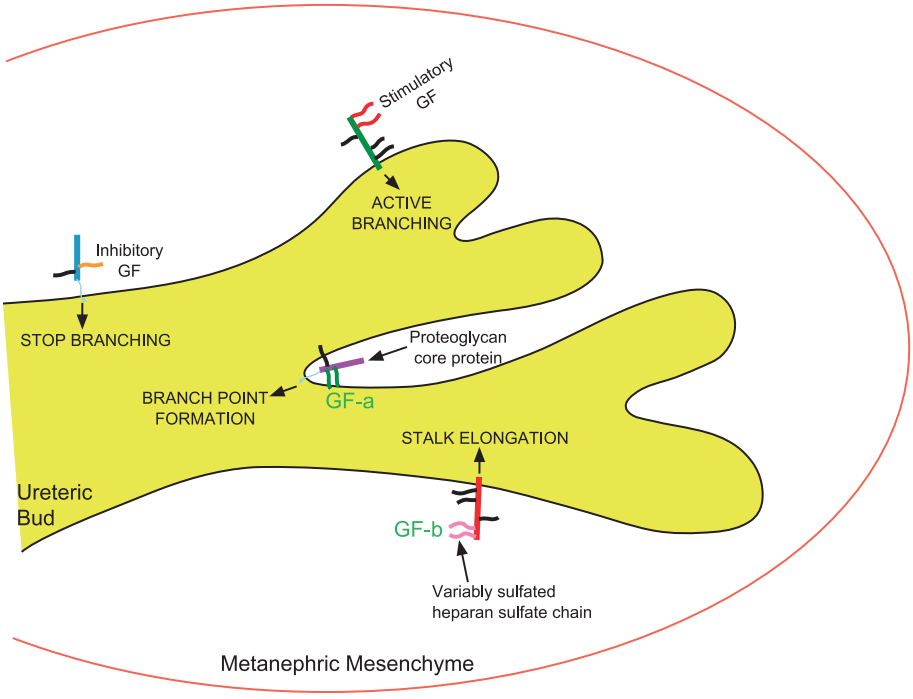

Fig. 12. Proposed model for the role of heparan sulfate proteoglycans in ureteric bud (UB) branching morphogenesis. The molecular diversity of HSPGs [various core protein isoforms and variable length and sulfation of the heparan sulfate (HS) chain] may allow for spatiotemporal modulation of the morphogen signal, including the creation of growth factor gradients. For example, in this cartoon, the binding of growth factor-a (GF-a) to a unique HSPG (colors represent unique core protein–variably sulfated HS combinations) results in branch point formation while the binding of growth factor-b (GF-b) to another HSPG leads to stalk elongation. Heparan sulfate proteoglycans (HSPG) interact with many stimulatory (growth/branch-promoting) and inhibitory (growth/branch-inhibiting) factors (see text for details). HSPGs may mediate the transition from a stage characterized by active growth and branching to a stage in which branching ceases through the differential binding of stimulatory and inhibitory growth factors (GF), effectively creating a "switch" between different stages of branching. For example, near the tips of the UB, HSPGs may modulate growth and branch promoting signals to propel the branching epithelium forward. However, at the stalks of the UB, HSPGs may modulate inhibitory signals to prevent further budding and maintain tubule caliber. This transition may occur through a change in core protein expression (e.g., syndecan to glypican) or through a change in HS sulfation pattern (predominant 6-O-sulfation to predominant N-sulfation). Different HS chains on the same protein core may be able to modulate these signals allowing for fine-tuning of these signals even at the cellular level. Not shown are postulated growth factor gradients that may be HS dependent.

These events likely occur through creation of growth factor gradients and regulation of growth factor–receptor binding, the specificity of which is dictated by the HS moieties. These microenvironments are likely dynamic and are modified based on the growth factor milieu and stage of development. As a result, the expression of protein cores with variably sulfated GAGs may, along with stage-specific heparin-binding growth factors, act as a switch to transition the developing collecting system from one stage of branching morphogenesis (e.g., rapid UB growth and branching) to another (e.g., slowing down of branching) through the regulated signaling of branch promoting and branch inhibitory factors. Although this is a simplified view of an extremely complex system, one can begin to envision how HSPGs are central to UB branching morphogenesis and how PG-mediated control of a developmental process provides the ''fine tuning'' necessary to instruct the complex interactions that result in the development of a specific organ.

Acknowledgments

This work was supported by National Research Service Award 1F32DK09974 (to D.L.S.), National Institute of Diabetes and Digestive and Kidney Diseases Grants RO1-DK49517 and RO1-DK57286 (to S.K.N), RO1-GM33063 (to J.D.E.), and an American Heart Association Scientist Development Award 9730096N (to K.T.B). K.T. Bush is also supported by a Normon S. Coplon Extramural Grant from Satellite Healthcare, Inc. The care and use of the animals described in this investigation conform to the procedures of the laboratory's animal protocol approved by the Animal Subjects Program and the IACUC of the University of California, San Diego. The authors thank Dr. Hiro Sakurai for his critical reading of this manuscript.

References

Alexander, C.M., Reichsman, F., Hinkes, M.T., Lincecum, J., Becker, K.A., Cumberledge, S., Bernfield, M., 2000. Syndecan-1 is required for Wnt-1-induced mammary tumorigenesis in mice. Nat. Genet. 25, 329–332.

Allen, B.L., Filla, M.S., Rapraeger, A.C., 2001. Role of heparan sulfate as a tissue-specific regulator of FGF-4 and FGF receptor recognition. J. Cell Biol. 155, 845–858.

Ameye, L., Young, M.F., 2002. Mice deficient in small leucine-rich proteoglycans: novel in vivo models for osteoporosis, osteoarthritis, Ehlers–Danlos syndrome, muscular dystrophy, and corneal diseases. Glycobiology 12, 107R–116R.

Arikawa-Hirasawa, E., Watanabe, H., Takami, H., Hassell, J.R., Yamada, Y., 1999. Perlecan is essential for cartilage and cephalic development. Nat. Genet. 23, 354–358.

Bai, X., Crawford, B., Esko, J.D., 2001. Selection of glycosaminoglycan-deficient mutants. Methods Mol. Biol. 171, 309–316.

Barnett, M.W., Fisher, C.E., Perona-Wright, G., Davies, J.A., 2002. Signalling by glial cell line-derived neurotrophic factor (GDNF) requires heparan sulphate glycosaminoglycan. J. Cell Sci. 115, 4495–4503.

Brenner, B.M., Garcia, D.L., Anderson, S., 1988. Glomeruli and blood pressure. Less of one, more the other? Am. J. Hypertens. 1, 335–347.

Bullock, S.L., Fletcher, J.M., Beddington, R.S., Wilson, V.A., 1998. Renal agenesis in mice homozygous for a gene trap mutation in the gene encoding heparan sulfate 2-sulfotransferase. Genes Dev. 12, 1894–1906.

Bush, K.T., Stuart, R.O., Nigam, S.K., 2003. Developmental biology of the kidney. In: Brenner, B.M. (Ed.), The Kidney, seventh ed. Saunders, Philadelphia, pp. 73–103.

Bush, K.T., Sakurai, H., Steer, D.L., Leonard, M.O., Sampogna, R.V., Meyer, T.N., Schwesinger, C., Qiao, J., Nigam, S.K., 2004. TGF-beta superfamily members modulate growth, branching, shaping, and patterning of the ureteric bud. Dev. Biol. 266, 285–298.

Cancilla, B., Ford-Perriss, M.D., Bertram, J.F., 1999. Expression and localization of fibroblast growth factors and fibroblast growth factor receptors in the developing rat kidney. Kidney Int. 56, 2025–2039.

Cano-Gauci, D.F., Song, H.H., Yang, H., McKerlie, C., Choo, B., Shi, W., Pullano, R., Piscione, T.D., Grisaru, S., Soon, S., Sedlackova, L., Tanswell, A.K., Mak, T.W., Yeger, H., Lockwood, G.A., Rosenblum, N.D., Filmus, J., 1999. Glypican-3-deficient mice exhibit developmental overgrowth and some of the abnormalities typical of Simpson–Golabi–Behmel syndrome. J. Cell Biol. 146, 255–264.

Clayton, A., Thomas, J., Thomas, G.J., Davies, M., Steadman, R., 2001. Cell surface heparan sulfate proteoglycans control the response of renal interstitial fibroblasts to fibroblast growth factor-2. Kidney Int. 59, 2084–2094.

Costell, M., Gustafsson, E., Aszodi, A., Morgelin, M., Bloch, W., Hunziker, E., Addicks, K., Timpl, R., Fassler, R., 1999. Perlecan maintains the integrity of cartilage and some basement membranes. J. Cell Biol. 147, 1109–1122.

Danielson, K.G., Baribault, H., Holmes, D.F., Graham, H., Kadler, K.E., Iozzo, R.V., 1997. Targeted disruption of decorin leads to abnormal collagen fibril morphology and skin fragility. J. Cell Biol. 136, 729–743.

Davies, J., Lyon, M., Gallagher, J., Garrod, D., 1995. Sulphated proteoglycan is required for collecting duct growth and branching but not nephron formation during kidney development. Development 121, 1507–1517.

Echtermeyer, F., Streit, M., Wilcox-Adelman, S., Saoncella, S., Denhez, F., Detmar, M., Goetinck, P., 2001. Delayed wound repair and impaired angiogenesis in mice lacking syndecan-4. J. Clin. Invest. 107, R9–R14.

Esko, J.D., Weinke, J.L., Taylor, W.H., Ekborg, G., Roden, L., Anantharamaiah, G., Gawish, A., 1987. Inhibition of chondroitin and heparan sulfate biosynthesis in Chinese hamster ovary cell mutants defective in galactosyltransferase I. J. Biol. Chem. 262, 12189–12195.

Faham, S., Linhardt, R.J., Rees, D.C., 1998. Diversity does make a difference: fibroblast growth factor–heparin interactions. Curr. Opin. Struct. Biol. 8, 578–586.

Fritz, T.A., Lugemwa, F.N., Sarkar, A.K., Esko, J.D., 1994. Biosynthesis of heparan sulfate on beta-D-xylosides depends on aglycone structure. J. Biol. Chem. 269, 300–307.

Gautam, M., Noakes, P.G., Moscoso, L., Rupp, F., Scheller, R.H., Merlie, J.P., Sanes, J.R., 1996. Defective neuromuscular synaptogenesis in agrin-deficient mutant mice. Cell 85, 525–535.

Gotte, M., Joussen, A.M., Klein, C., Andre, P., Wagner, D.D., Hinkes, M.T., Kirchhof, B., Adamis, A.P., Bernfield, M., 2002. Role of syndecan-1 in leukocyte–endothelial interactions in the ocular vasculature. Invest. Ophthalmol. Visual Sci. 43, 1135–1141.

Greve, H., Cully, Z., Blumberg, P., Kresse, H., 1988. Influence of chlorate on proteoglycan biosynthesis by cultured human fibroblasts. J. Biol. Chem. 263, 12886–12892.

Grisaru, S., Cano-Gauci, D., Tee, J., Filmus, J., Rosenblum, N.D., 2001. Glypican-3 modulates BMP- and FGF-mediated effects during renal branching morphogenesis. Dev. Biol. 231, 31–46.

Humphries, D.E., Silbert, J.E., 1988. Chlorate: a reversible inhibitor of proteoglycan sulfation. Biochem. Biophys. Res. Commun. 154, 365–371.

Ishiguro, K., Kadomatsu, K., Kojima, T., Muramatsu, H., Tsuzuki, S., Nakamura, E., Kusugami, K., Saito, H., Muramatsu, T., 2000. Syndecan-4 deficiency impairs focal adhesion formation only under restricted conditions. J. Biol. Chem. 275, 5249–5252.

Ishiguro, K., Kadomatsu, K., Kojima, T., Muramatsu, H., Matsuo, S.,

Kusugami, K., Saito, H., Muramatsu, T., 2001. Syndecan-4 deficiency increases susceptibility to kappa-carrageenan-induced renal damage. Lab. Invest. 81, 509–516.

Kispert, A., Vainio, S., Shen, L., Rowitch, D.H., McMahon, A.P., 1996. Proteoglycans are required for maintenance of Wnt-11 expression in the ureter tips. Development 122, 3627–3637.

Koseki, C., Herzlinger, D., al-Awqati, Q., 1992. Apoptosis in metanephric development. J. Cell Biol. 119, 1327–1333.

Krufka, A., Guimond, S., Rapraeger, A.C., 1996. Two hierarchies of FGF-2 signaling in heparin: mitogenic stimulation and high-affinity binding/receptor transphosphorylation. Biochemistry 35, 11131–11141.

Laitinen, L., Virtanen, I., Saxen, L., 1987. Changes in the glycosylation pattern during embryonic development of mouse kidney as revealed with lectin conjugates. J. Histochem. Cytochem. 35, 55–65.

Lash, J.W., Saxen, L., Ekblom, P., 1983. Biosynthesis of proteoglycans in organ cultures of developing kidney mesenchyme. Exp. Cell Res. 147, 85–93.

Lelongt, B., Makino, H., Dalecki, T.M., Kanwar, Y.S., 1988. Role of proteoglycans in renal development. Dev. Biol. 128, 256–276.

Lugemwa, F.N., Esko, J.D., 1991. Estradiol beta-D-xyloside, an efficient primer for heparan sulfate biosynthesis. J. Biol. Chem. 266, 6674–6677.

Lyon, M., Gallagher, J.T., 1998. Bio-specific sequences and domains in heparan sulphate and the regulation of cell growth and adhesion. Matrix Biol. 17, 485–493.

Merry, C.L., Bullock, S.L., Swan, D.C., Backen, A.C., Lyon, M., Beddington, R.S., Wilson, V.A., Gallagher, J.T., 2001. The molecular phenotype of heparan sulfate in the Hs2st−/− mutant mouse. J. Biol. Chem. 276, 35429–35434.

Meyer, T.N., Schwesinger, C., Bush, K.T., Stuart, R.O., Rose, D.W., Shah, M.M., Vaughn, D.A., Steer, D.L., Nigam, S.K., Spatiotemporal regulation of morphogenetic molecules during in vitro branching of the isolated ureteric bud. Dev Biol., submitted for publication.

Mjaatvedt, C.H., Yamamura, H., Capehart, A.A., Turner, D., Markwald, R.R., 1998. The Cspg2 gene, disrupted in the hdf mutant, is required for right cardiac chamber and endocardial cushion formation. Dev. Biol. 202, 56–66.

Mugrauer, G., Ekblom, P., 1991. Contrasting expression patterns of three members of the myc family of protooncogenes in the developing and adult mouse kidney. J. Cell Biol. 112, 13–25.

Nakato, H., Kimata, K., 2002. Heparan sulfate fine structure and specificity of proteoglycan functions. Biochim. Biophys. Acta 1573, 312–318.

Nigam, S.K., 1995. Determinants of branching tubulogenesis. Curr. Opin. Nephrol. Hypertens. 4, 209–214.

Nigam, S.K., 2003. From the ureteric bud to the penome. Kidney Int. 64, 2320–2322.

Ornitz, D.M., 2000. FGFs, heparan sulfate and FGFRs: complex interactions essential for development. BioEssays 22, 108–112.

Perrimon, N., Bernfield, M., 2000. Specificities of heparan sulphate proteoglycans in developmental processes. Nature 404, 725–728.

Pilia, G., Hughes-Benzie, R.M., MacKenzie, A., Baybayan, P., Chen, E.Y., Huber, R., Neri, G., Cao, A., Forabosco, A., Schlessinger, D., 1996. Mutations in GPC3, a glypican gene, cause the Simpson–Golabi–Behmel overgrowth syndrome. Nat. Genet. 12, 241–247.

Platt, J.L., Brown, D.M., Granlund, K., Oegema, T.R., Klein, D.J., 1987. Proteoglycan metabolism associated with mouse metanephric development: morphologic and biochemical effects of beta-D-xyloside. Dev. Biol. 123, 293–306.

Platt, J.L., Trescony, P., Lindman, B., Oegema, T.R., 1990. Heparin and heparan sulfate delimit nephron formation in fetal metanephric kidneys. Dev. Biol. 139, 338–348.

Pohl, M., Sakurai, H., Bush, K.T., Nigam, S.K., 2000a. Matrix metalloproteinases and their inhibitors regulate in vitro ureteric bud branching morphogenesis. Am. J. Physiol.: Renal Physiol. 279, F891–F900.

Pohl, M., Stuart, R.O., Sakurai, H., Nigam, S.K., 2000b. Branching morphogenesis during kidney development. Annu. Rev. Physiol. 62, 595–620.

Pye, D.A., Vives, R.R., Turnbull, J.E., Hyde, P., Gallagher, J.T., 1998. Heparan sulfate oligosaccharides require 6-O-sulfation for promotion of basic fibroblast growth factor mitogenic activity. J. Biol. Chem. 273, 22936–22942.

Qiao, J., Sakurai, H., Nigam, S.K., 1999. Branching morphogenesis independent of mesenchymal–epithelial contact in the developing kidney. Proc. Natl. Acad. Sci. U. S. A. 96, 7330–7335.

Qiao, J., Bush, K.T., Steer, D.L., Stuart, R.O., Sakurai, H., Wachsman, W., Nigam, S.K., 2001. Multiple fibroblast growth factors support growth of the ureteric bud but have different effects on branching morphogenesis. Mech. Dev. 109, 123–135.

Rapraeger, A.C., Krufka, A., Olwin, B.B., 1991. Requirement of heparan sulfate for bFGF-mediated fibroblast growth and myoblast differentiation. Science 252, 1705–1708.

Reizes, O., Lincecum, J., Wang, Z., Goldberger, O., Huang, L., Kaksonen, M., Ahima, R., Hinkes, M.T., Barsh, G.S., Rauvala, H., Bernfield, M., 2001. Transgenic expression of syndecan-1 uncovers a physiological control of feeding behavior by syndecan-3. Cell 106, 105–116.

Rickard, S.M., Mummery, R.S., Mulloy, B., Rider, C.C., 2003. The binding of human glial cell line-derived neurotrophic factor (GDNF) to heparin and heparan sulphate: importance of 2-O-sulphate groups and effect on its interaction with its receptor GFR{alpha}1. Glycobiology 6, 6.

Safaiyan, F., Kolset, S.O., Prydz, K., Gottfridsson, E., Lindahl, U., Salmivirta, M., 1999. Selective effects of sodium chlorate treatment on the sulfation of heparan sulfate. J. Biol. Chem. 274, 36267–36273.

Sakurai, H., Nigam, S.K., 1997. Transforming growth factor-beta selectively inhibits branching morphogenesis but not tubulogenesis. Am. J. Physiol. 272, F139–F146.

Sakurai, H., Barros, E.J., Tsukamoto, T., Barasch, J., Nigam, S.K., 1997. An in vitro tubulogenesis system using cell lines derived from the embryonic kidney shows dependence on multiple soluble growth factors. Proc. Natl. Acad. Sci. U. S. A. 94, 6279–6284.

Sakurai, H., Bush, K.T., Nigam, S.K., 2001. Identification of pleiotrophin as a mesenchymal factor involved in ureteric bud branching morphogenesis. Development 128, 3283–3293.

Sanchez, M.P., Silos-Santiago, I., Frisen, J., He, B., Lira, S.A., Barbacid, M., 1996. Renal agenesis and the absence of enteric neurons in mice lacking GDNF. Nature 382, 70–73.

Santos, O.F., Nigam, S.K., 1993. HGF-induced tubulogenesis and branching of epithelial cells is modulated by extracellular matrix and TGF-beta. Dev. Biol. 160, 293–302.

Schwartz, N.B., Galligani, L., Ho, P.L., Dorfman, A., 1974. Stimulation of synthesis of free chondroitin sulfate chains by beta-D-xylosides in cultured cells. Proc. Natl. Acad. Sci. U. S. A. 71, 4047–4051.

Shah, M.M., Sampogna, R.V., Sakurai, H., Bush, K.T., Nigam, S.K., 2004. Branching morphogenesis and kidney disease. Development 131, 1449–1462.

Steer, D.L., Fukuoka, K., Mendoza, S., Nigam, S.K., 2004. Development of the genitourinary system. In: Epstein, C.J., Erickson, R.P., Wynshaw Boris, A. (Eds.), Inborn Errors of Development. Oxford Univ. Press, New York, pp. 168–181.

Stuart, R.O., Barros, E.J., Ribeiro, E., Nigam, S.K., 1995. Epithelial tubulogenesis through branching morphogenesis: relevance to collecting system development. J. Am. Soc. Nephrol. 6, 1151–1159.

Stuart, R.O., Bush, K.T., Nigam, S.K., 2001. Changes in global gene expression patterns during development and maturation of the rat kidney. Proc. Natl. Acad. Sci. U. S. A. 98, 5649–5654.

Stuart, R.O., Bush, K.T., Nigam, S.K., 2003. Changes in gene expression patterns in the ureteric bud and metanephric mesenchyme in models of kidney development. Kidney Int. 64, 1997–2008.

The, I., Bellaiche, Y., Perrimon, N., 1999. Hedgehog movement is regulated through tout velu-dependent synthesis of a heparan sulfate proteoglycan. Mol. Cell 4, 633–639.

Tumova, S., Woods, A., Couchman, J.R., 2000. Heparan sulfate proteoglycans on the cell surface: versatile coordinators of cellular functions. Int. J. Biochem. Cell Biol. 32, 269–288.

Vainio, S., Jalkanen, M., Bernfield, M., Saxen, L., 1992. Transient expres-

sion of syndecan in mesenchymal cell aggregates of the embryonic kidney. Dev. Biol. 152, 221–232.

Whitelock, J.M., Murdoch, A.D., Iozzo, R.V., Underwood, P.A., 1996. The degradation of human endothelial cell-derived perlecan and release of bound basic fibroblast growth factor by stromelysin, collagenase, plasmin, and heparanases. J. Biol. Chem. 271, 10079–10086.

Xu, T., Bianco, P., Fisher, L.W., Longenecker, G., Smith, E., Goldstein, S., Bonadio, J., Boskey, A., Heegaard, A.M., Sommer, B., Satomura, K., Dominguez, P., Zhao, C., Kulkarni, A.B., Robey, P.G., Young, M.F., 1998. Targeted disruption of the biglycan gene leads to an osteoporosis-like phenotype in mice. Nat. Genet. 20, 78–82.

Yayon, A., Klagsbrun, M., Esko, J.D., Leder, P., Ornitz, D.M., 1991. Cell surface, heparin-like molecules are required for binding of basic fibroblast growth factor to its high affinity receptor. Cell 64, 841–848.

Yu, W.H., Woessner Jr., J.F., 2000. Heparan sulfate proteoglycans as extracellular docking molecules for matrilysin (matrix metalloproteinase 7). J. Biol. Chem. 275, 4183–4191.

Zent, R., Bush, K.T., Pohl, M.L., Quaranta, V., Koshikawa, N., Wang, Z., Kreidberg, J.A., Sakurai, H., Stuart, R.O., Nigam, S.K., 2001. Involvement of laminin binding integrins and laminin-5 in branching morphogenesis of the ureteric bud during kidney development. Dev. Biol. 238, 289–302.